

## Accepted Manuscript

Title: Ultrasound assisted rare earth doped Wollastonite nanopowders: Labeling agent for imaging eccrine latent fingerprints and cheiloscopy applications

Authors: R.B. Basavaraj, H. Nagabhushana, G.P. Darshan, B. Daruka Prasad, S.C. Sharma, K.N. Venkatachalaiah



PII: S1226-086X(17)30092-8  
DOI: <http://dx.doi.org/doi:10.1016/j.jiec.2017.02.019>  
Reference: JIEC 3300

To appear in:

Received date: 1-10-2016  
Revised date: 28-1-2017  
Accepted date: 27-2-2017

Please cite this article as: R.B.Basavaraj, H.Nagabhushana, G.P.Darshan, B.Daruka Prasad, S.C.Sharma, K.N.Venkatachalaiah, Ultrasound assisted rare earth doped Wollastonite nanopowders: Labeling agent for imaging eccrine latent fingerprints and cheiloscopy applications, Journal of Industrial and Engineering Chemistry <http://dx.doi.org/10.1016/j.jiec.2017.02.019>

This is a PDF file of an unedited manuscript that has been accepted for publication. As a service to our customers we are providing this early version of the manuscript. The manuscript will undergo copyediting, typesetting, and review of the resulting proof before it is published in its final form. Please note that during the production process errors may be discovered which could affect the content, and all legal disclaimers that apply to the journal pertain.

<AT>Ultrasound assisted rare earth doped Wollastonite nanopowders: Labeling agent for imaging eccrine latent fingerprints and cheiloscropy applications

<AU>R.B. Basavaraj<sup>a</sup>, H.Nagabhushana<sup>a\*</sup> ##Email##bhushanvlc@gmail.com##/Email##, G.P. Darshan<sup>b</sup>, B.Daruka Prasad<sup>c</sup>, S.C.Sharma<sup>d</sup>, K.N.Venkatachalaiah<sup>e</sup>  
<AU>

<AFF><sup>a</sup>Prof. C.N.R. Rao Centre for Advanced Materials Research, Tumkur University *Tumkur 572 103, India*

<AFF><sup>b</sup>Department of Physics, Acharya Institute of Graduate Studies, Bangalore 560 107, India

<AFF><sup>c</sup>Department of Physics, BMS Institute of Technology and Management, VTU- Belagavi affiliated, Bangalore 560 064, India

<AFF><sup>d</sup>Professor, Department of Mechanical Engineering, Jain University, Advisor, Jain group of Institutions, Bangalore, India

<AFF><sup>e</sup>Amrita School of Engineering, Bangalore Campus, Amrita Vishwa-vidyapeetam, Bengaluru-560035, *India*.

<PA>+91- 9945954010.

<ABS-Head><ABS-HEAD>Graphical abstract

<ABS-P>

<ABS-P><xps:span class="xps\_Image">fx1</xps:span>

<ABS-HEAD>Highlights ► Nano CdSiO<sub>3</sub>:Dy<sup>3+</sup> powders were fabricated using modified sonochemical method. ► Compounds were used to enhance eccrine latent finger print and lips prints qualities. ► Surface morphologies were studied with different sonication influential parameters. ► Prepared compounds were useful for near ultraviolet white light emitting diodes.

<ABS-HEAD>**Abstract**

<ABS-P>Nano research offered new possibilities in surface-based science includes latent fingerprints and lips print detection on various surfaces. CdSiO<sub>3</sub>:Dy<sup>3+</sup> nanopowders were fabricated via modified sonochemical method. Eccrine prints stained by optimized composition of prepared samples, exhibited high sensitivity, low background hindrance on various surfaces compared to traditional fluorescent powders. Surface morphologies were studied with different sonication influential parameters. Average crystallites size and band gap were 22 nm and 5.37 eV respectively. Photometric CIE and CCT values were close to near ultraviolet light with CP of 95% for the prepared compounds confirms their utility in the field of optoelectronics.

<KWD>Keywords: Eccrine latent fingerprint; ultrasound synthesis; color hindrance;

Photoluminescence.

<H1>1. Introduction

In the recent years, rare earth (RE) doped luminescent nanophosphors have been used as a labeling materials for fingerprint recognition due to their smaller crystallite size and enormous control on the adhesion competence to eccrine latent fingerprints (LFPs) [1 - 4]. Therefore, use of RE doped nanomaterials as staining agent in LFPs detection has stimulated the materials scientists.

Furthermore, it was well documented that the RE doped ions such as  $\text{Eu}^{3+}$ ,  $\text{Gd}^{3+}$ ,  $\text{Sm}^{3+}$ ,  $\text{Dy}^{3+}$  were biocompatible and relatively less harmful [5-9].

Generally LFPs at crime scenes were normally invisible or poorly visible to investigators were enhanced using conventional non-fluorescent powders [10-12]. Powder dusting method was most frequently adopted technique for developing LFPs in Forensic science [13-15]. This method has several problems such as low sensitivity, low contrast, high background interference and high auto fluorescence interference [16-18]. In order to overcome with these difficulties, research in nano science and technology offers surface-based science including fingerprint detection on smooth surfaces, single background colour, multiple background color and strong background auto fluorescence etc. [19, 20]. Nano metal oxides [21], Aluminates [22, 23], RE doped  $\text{Gd}_2\text{O}_3$  nanomaterials [24], Titanium oxide ( $\text{TiO}_2$ ) [25], CdSe [26], and  $\text{SiO}_2/\text{Eu}^{3+}$  [27] material were employed for the effective reveal of eccrine LFPs. Majority of these materials requires complicated synthesis routes; therefore in some occasions they are not suitable for frequent use at crime spots. Silicates were found to be effective luminescent materials due to their stable crystal structure, outstanding long term durability and strong absorption in the near-UV region. Further, silicate based phosphors exhibit better properties such as thermally stable, wide energy band gap, and high resistance over acid, alkali and oxygen [28-33]. Traditionally, silicates were prepared at high temperature solid state method ( $>1000\text{ }^\circ\text{C}$ ) for several hours and the final product leads to irregular particles size and large defects which were not suitable for solid state lighting applications. Among the other methods, ultrasound sonication is treated as simple and effective. In this method, series of chemical reactions arises from acoustic cavitation which results for the formation, growth as well as sudden collapse of bubbles in the solution. As per the hot-spot theory, a very high temperature was able to collapse the bubbles within nanoseconds. This along with the use of surfactants can tune the size distribution, shape and size of the powders more effectively. In order to obtain nano/micro structured materials at sensibly low temperature was extremely indispensable for industrial applications via ultrasound route [34 - 38].

Till date, no reports are available for the preparation of  $\text{CdSiO}_3:\text{Dy}^{3+}$  nanopowders (NPs) via ultrasonic process. Effect of preparation method and formation temperature to obtain different morphologies of Pure and  $\text{Dy}^{3+}$  doped  $\text{CdSiO}_3$  compounds were listed in **Table.1** [39-43]. Herein, we report ultrasonic sonochemical synthesized  $\text{Dy}^{3+}$  (5 mol %) doped  $\text{CdSiO}_3$  host lattice for developing eccrine latent fingerprint and lips print applications on infiltrating and non- infiltrating surfaces of various kinds of materials. The effective use of prepared compound displayed well defined ridges without any background hindrance. In addition, the structural, morphological and photometric properties of prepared samples were reported systematically according to the flow chart shown in **Fig.1**.

## 2. Experimental

Chemicals and surfactants utilized in the present work along with their formula, structure, and molecular weight were listed in **Table.2**.  $\text{CdSiO}_3:\text{Dy}^{3+}$  (1-11 mol %) nanoparticles (NPs) were prepared by using ultrasound assisted sonochemical method in presence of surfactants. For the preparation of 1 mol % of  $\text{CdSiO}_3:\text{Dy}^{3+}$ , stoichiometric quantities of cadmium nitrate [ $(\text{Cd}(\text{NO}_3)_2$ ; 11.821 g], dysprosium nitrate [ $\text{Dy}(\text{NO}_3)_3$ ; 0.0348 g] and tetraethyl orthosilicate [ $\text{Si}(\text{OC}_2\text{H}_5)_4$ ; 10.41 ml] were well dissolved in 50 ml double distilled water and mixed thoroughly until a homogeneous

mixture was obtained. 5 g of starch was dissolved in 100 ml of distilled water and divided into different concentrations (5–30 ml). Initially 5 ml of starch solution was added to the above precursor solution and stirred for few minutes. The resultant solution was then subjected to the ultrasonication (frequency ~20 kHz, power ~300 W) at a fixed temperature of 60 °C and various reaction times from 1 h to 6 h. The final precipitate was filtered and washed several times by distilled water and ethanol. The resultant powder was dried at 60 °C for 3 h. Same procedure was repeated in presence of other surfactants such as CTAB, SDS and PEG. Effect of different parameters such as sonication time, pH, sonication power, surfactant, morphology and photoluminescence properties were studied. Further, prepared compounds were used for enhancing the quality of eccrine LFPs.

The powder X-ray diffraction (PXRD) measurements were performed on the diffractometer (Shimadzu 7000) with graphite monochromatized Cu-K $\alpha$  radiation ( $\lambda = 0.15406$  nm). The surface morphology was studied by Hitachi table top scanning electron microscope (Hitachi- TM 3000). Transmission electron microscope (Hitachi H-8100, Kevex sigma TM Quasar, USA) was used to study the crystallite size of the material. Spectrophotometer (Lambda – 35, PerkinElmer) was used to obtain the diffuse reflectance spectra and energy band gaps. Spectrofluorimeter equipped with Fluorolog-3 (Jobin Yvon) was utilized to measure the photoluminescence (PL).

<H1>3. Results and discussion

<H2>3.1. Revelation of eccrine LFPs using CdSiO<sub>3</sub>: Dy<sup>3+</sup> (5 mol %) NPs

Eccrine LFPs were collected from clean hands of single healthy donor by gently pressing on different surfaces with medium pressure at room temperature. The surfaces include infiltrating and non-infiltrating materials. Synthesized CdSiO<sub>3</sub>: Dy<sup>3+</sup> (5 mol %) NPs were applied carefully on eccrine LFPs and excess was removed by smooth brushing. LFPs were photographed using a Nikon D3100/AF-S Nikkor 50 mm f/2.8G ED lens digital camera under normal light and under 254 nm UV light. **Fig.2.** shows the schematic representation of the complete process.

<H2>3.2. Eccrine Latent LFPs detection using CdSiO<sub>3</sub>: Dy<sup>3+</sup> NPs

**Fig. 3** shows the observed eccrine LFPs on different forensic relevant non-porous materials (glass, stainless steel, aluminum foil; mobile screen, laptop screen and calling bell) after treated with the phosphor material. It was observed that the well- resolved minutiae ridges were identified on all the surfaces without any color hindrance. Hence it can be used as labeling materials for the detection of LFPs on forensic relevant non-porous surfaces. Further, LFPs were enhanced on different infiltrating materials namely magazine covers with dissimilar background colors (**Fig.4**). Interestingly, in all these cases, clearer ridge patterns were observed without any background interference. In the present method, it is possible to reveal the LFPs within 5 minutes hence it may be helpful for investigators for obtaining clues immediately. **Fig. 5** shows the LFPs stained by Dy<sup>3+</sup>

(5 mol %) doped CdSiO<sub>3</sub> NPs obtained using four different surfactants (Starch, CTAB, PEG and SDS). From the figure, it was observed that the starch assisted phosphor stained on eccrine LFPs exhibited better quality images without any background hindrance. This may be explained based on the egg box model where the single linear chain compound with many –OH ions makes the process of wrapping of starch organic compounds in simpler way than the others.

Identification of minutiae patterns in LFPs is extremely helpful to know the culprit. **Fig.6** shows the eccrine LFPs stained by starch assisted CdSiO<sub>3</sub>:Dy<sup>3+</sup> NPs, demonstrated a well-resolved ridge flow, pattern configuration and minutiae ridges (ridge termination, bifurcation, crossover, and etc.). This suggests that, there was a strong interaction between chemical constituent of eccrine LFPs and labeled powder. In a crime spots, incomplete LFPs may be regularly encountered. Identification of a victim by incomplete LFPs will not provide an important support for investigating agencies. LFPs obtained after stained by CdSiO<sub>3</sub>:Dy<sup>3+</sup> NPs on non-porous Indian rupee coin and bar codes exhibited maximum minutiae ridges (**Fig.7**).

In addition, reveal of lips print or cheiloscopy was also performed similar to that of LFP analysis [44-46]. Latent lips prints has many elevations and depressions leads to evidence in individual identification and criminal investigation at forensic dentistry. Usually, latent lips prints can be found where the surface in contact with the lips. The vermilion borders of lips have minor salivary and sebaceous glands contents present around the edges of the lip associated with hair follicles, sweat glands in between and secreting oils. The secretions and continual moisturizing by the tongue due to occasional sebaceous glands present on the lip, there are chances for the presence of the latent lip prints on the surfaces viz., glasses, cigarettes, straws, food items etc. However, some extra effort was required to make lip prints visible. Therefore, CdSiO<sub>3</sub>:Dy<sup>3+</sup> (5 mol %) NPs were utilized to develop latent lips prints on glass to exhibit efficiency and selectivity of the synthesized labeling NPs. **Fig.8 (a)** shows the three different lip prints stained by optimized CdSiO<sub>3</sub>:Dy<sup>3+</sup> NPs. From the figure, it was evident that Tsuchihashi's type 2 and type 1 well- defined lips print ridges were observed due to smaller and uniform sized powders as well as adhesive nature of the material (**Fig.8 (b)**).

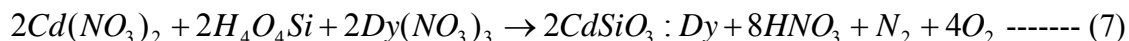
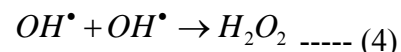
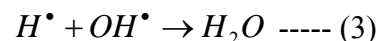
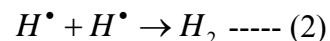
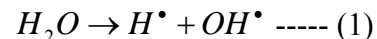
Successfully it was demonstrated that the prepared CdSiO<sub>3</sub>:Dy<sup>3+</sup> NPs employed as a labeling material to reveal LFPs and lips print on different surfaces. LFPs and lips prints revealed shows patterns with high efficiency and high sensitivity (because no color hindrance and chemical constituents can be observed due to smaller crystalline size). In addition, CdSiO<sub>3</sub>:Dy<sup>3+</sup> (5 mol %) NPs can be stored for longer time without any loss of luminescence efficiency.

### 3.3. Morphological analysis

The **Fig.9 (A)** shows the SEM micrographs of CdSiO<sub>3</sub>:Dy<sup>3+</sup> (5 mol %) NPs prepared using various concentrations of CTAB as surfactant under 6 h sonication time. At lower concentrations of CTAB (5 – 15 ml) (**Fig.9A (a – c)**), irregular flake like morphology was noticed. As the CTAB concentration was increased to 20 - 30 ml, flakes starts self-assembled (**Fig.9A (d – f)**). The present results clearly evident that morphology was highly dependent on the surfactant concentration. SEM micrographs of CdSiO<sub>3</sub>:Dy<sup>3+</sup> (5 mol %) NPs prepared for 6 h sonication time with starch as the surfactant (**Fig.9B**). When the starch concentration was 5 - 15 ml (**Fig.9B (a-c)**), an agglomerated

randomly distributed hexagonal pyramid shaped structures were observed. As the starch concentration was increased to 15 to 30 ml various sharp pyramids, flat hexagonal disk like particles were observed in **Fig.9B (d-f)**.

The reaction mechanism for the formation of CdSiO<sub>3</sub>:Dy<sup>3+</sup> (5 mol %) NPs during ultrasound was given below:



Eqs. (1) to (7) illustrates the formation of primary ions which have been formed by the dissociation of water, tetraethyl orthosilicate (TEOS), cadmium nitrate and dysprosium nitrate which further decomposes to give primary nano particles of CdSiO<sub>3</sub>:Dy<sup>3+</sup>. During the reaction time the starch particles experience the following process:

<remove picture pageno 9>Starch particles hydration of starch + leaching of amylose ---- (8)

<remove picture pageno 9>Amylose (glue) + CdSiO<sub>3</sub>:Dy<sup>3+</sup> nuclei clumping of CdSiO<sub>3</sub>: Dy into hexagonal blocks --- (9)

Eqs. (7) and (8) demonstrates that in existence of water and sonication irradiation, starch particles endures gelatinization [47] as a result hydration of starch particles leaching out of amylose and some of them gets collapsed. Subsequently after 6 h of sonication temperature of solution which primarily was 30 °C reaches 60 °C which favors gelatinization. Amylose which comes out has a sticking property it binds onto CdSiO<sub>3</sub> nuclei resulting in various shapes as amylose itself has affinity to form coil. When reaction mixture gets cooled these amylose units along with amylopectin and distorted starch particles form hydrogen bonds among them sticking nanoparticles composed into a hexagonal discs and pyramidal structures as depicted in **Fig. 10**.

**Fig. 11 (A)** shows the SEM micrographs of CdSiO<sub>3</sub>:Dy<sup>3+</sup> (5 mol %) NPs synthesized with different concentration of SDS (5, 10, 15, 20, 25 and 30 ml) with 6 h of ultrasonic irradiation time.

Here granular like structures were obtained which are solely dependent on the concentrations of

SDS surfactant. Initially, the granules were well separated with each other. As the SDS concentration was increased, these granules assembled together to form a honeycomb like structure. The change in morphology of the material was due to the trapping of primary particles of CdSiO<sub>3</sub> into the anionic surfactant SDS. Polyethylene glycol is polyether compound having wide range of applications in industrial and medicine. Due to its chain length effect and polymerization process PEG plays a vital role in surface modification of the nanomaterials. The effect of pH on the morphology of the obtained product was also studied in detail. **Fig.11 (B)** shows the SEM micrographs of CdSiO<sub>3</sub>:Dy<sup>3+</sup> (5 mol %) NPs prepared with different pH values under 3 h sonication time with starch surfactant (25 ml). The pH of the solution can be varied by adding HCl to the precursor solution. The leached out amylose during the gelatinization of the starch under ultrasonic irradiation with different pH values, will binds onto the primary CdSiO<sub>3</sub> nano cluster and forms a network like morphology of the agglomerated particles which bound to each other (**Fig.11 B**). These results were clearly evident that, pH of the precursor solution also influences on the morphology of the obtained product.

Fig. **12** shows the TEM images of optimized CdSiO<sub>3</sub>:Dy<sup>3+</sup> (5 mol %) NPs prepared with different surfactants and 6 h of ultrasonic irradiation time. It was clearly seen that TEM images were in good agreement with the morphology obtained in SEM micrographs and the crystallite size were in nano regime (20-40 nm) matches well with values estimated from Scherrer and W-H approaches.

### 3.4. Powder X-ray diffraction (PXRD) analysis

Fig. **13** shows the PXRD patterns of starch assisted pure CdSiO<sub>3</sub> NPs prepared by conventional mechanical stirring and ultrasonic method processed at 60 °C for 6 h irradiation time. It was clearly noticed that, small impurity peaks were identified due to the incomplete phase formation during

conventional stirring process. On the other hand, spectra exhibit sharp peaks belong to single monoclinic phase of CdSiO<sub>3</sub> NPs synthesized by ultrasonic method and well matched with the standard JCPDS. No.35-0810 [40]. The PXRD profile of the synthesized material under ultrasound method exhibit more intense peak and appreciable line broadening as compared to conventional stirring method (shown in blue circle in Fig.13). Diffraction peaks were well matched with standard JCPDS.No. 35-0810. The crystallite size and micro-strain of CdSiO<sub>3</sub>:Dy<sup>3+</sup> (5 mol %) with different reaction parameters were estimated by using Debye Scherrer's (D-S) formula and Williamson Hall (W-H) plots and the were tabulated in Table.3.

#### <H2>3.4. Diffuse reflectance spectra

Fig. **14(a)** shows the diffuse reflectance spectra (DRS) of Dy<sup>3+</sup> (1-11 mol %) doped CdSiO<sub>3</sub> NPs recorded in the range of 200 – 1100 nm at room temperature. The spectra exhibit weak absorption band at lower wavelength due to the metastable states formed between the conduction and valence bands of dysprosium ions. Various electronic absorption bands were also observed at longer wavelengths. The peaks at 320, 348, 364, 381, 796, 887, 1071 nm were attributes to <sup>6</sup>H<sub>15/2</sub> → <sup>4</sup>I<sub>11/2</sub>, <sup>6</sup>H<sub>15/2</sub> → <sup>6</sup>P<sub>7/2</sub>, <sup>6</sup>H<sub>15/2</sub> → <sup>4</sup>I<sub>13/2</sub>, <sup>6</sup>H<sub>15/2</sub> → <sup>6</sup>F<sub>5/2</sub>, <sup>6</sup>H<sub>5/2</sub> → <sup>6</sup>F<sub>7/2</sub> and <sup>6</sup>H<sub>5/2</sub> → <sup>6</sup>F<sub>9/2</sub> + <sup>6</sup>H<sub>7/2</sub> respectively. The red shifting of bands in the DRS were also observed due to the variation in the crystallite size and increase of dysprosium ions into the host matrix [48, 49].

The Kubelka–Munk (K-M) theory was employed to evaluate the energy band gaps of CdSiO<sub>3</sub>:Dy<sup>3+</sup> (1-11 mol %) NPs using DR spectra as shown in **Fig.14 (b)** [50]. The energy band gap values were evaluated and were summarized in Table 3. It was observed from the **Fig.14 (b)**, the energy band gap decreased as the dopant (Dy<sup>3+</sup>) concentration was increased (5.29–5.17 eV). The various structural order and disorder along with the different experimental conditions were responsible for the change energy band gap in the product. The refractive index of the obtained NPs was estimated by using the relation [51].

$$\frac{n_r^2 - 1}{n_r^2 + 1} = 1 - \sqrt{\frac{E_g}{20}} \text{ ----- (10)}$$



The refractive index of CdSiO<sub>3</sub>:Dy<sup>3+</sup> prepared under various reaction conditions were calculated by using the above relation and the values were listed in Table 3. It was evident from the table that, the refractive index of the material varies with dysprosium concentration in host lattice.

### <H2>3.5. Photoluminescence (PL) studies

The PL excitation spectrum of CdSiO<sub>3</sub>: Dy<sup>3+</sup> (5 mol %) NPs by keeping emission wavelength at 575 nm are shown in **Fig. 15 (a)**. The excitation spectrum comprise of sharp peaks at ~ 344, 381, 420, 450 and 465 nm were due to f-f transitions of Dy<sup>3+</sup> ions and were attributed to <sup>6</sup>H<sub>15/2</sub>→<sup>6</sup>P<sub>7/2</sub>, <sup>6</sup>H<sub>15/2</sub>→<sup>4</sup>I<sub>13/2</sub>, <sup>6</sup>H<sub>15/2</sub>→<sup>4</sup>G<sub>11/2</sub>, <sup>6</sup>H<sub>15/2</sub>→<sup>4</sup>I<sub>15/2</sub>, and <sup>6</sup>H<sub>15/2</sub>→<sup>4</sup>F<sub>9/2</sub> transitions respectively. **Fig.15 (b)** shows the emission spectra of doped CdSiO<sub>3</sub>: Dy<sup>3+</sup> (1-11 mol %) NPs excited at 344 nm. The emission spectra exhibits peaks in three regions i.e., blue (~ 465–500 nm) and yellow (~ 555–600 nm) and a weaker red emission region (~ 650- 700 nm). The peaks at 480 (blue), 575 (yellow) and 637 nm (red) were attributed to <sup>4</sup>F<sub>9/2</sub>→<sup>6</sup>H<sub>15/2</sub>, <sup>4</sup>F<sub>9/2</sub>→<sup>6</sup>H<sub>13/2</sub> and <sup>4</sup>F<sub>9/2</sub>→<sup>6</sup>H<sub>11/2</sub> transitions respectively. The peaks at 480 nm (<sup>4</sup>F<sub>9/2</sub>→<sup>6</sup>H<sub>15/2</sub>) and 575 nm (<sup>4</sup>F<sub>9/2</sub>→<sup>6</sup>H<sub>13/2</sub>) were due to magnetic dipole (MD) and electric dipole (ED) transition respectively [36]. The degree of distortion from the inversion symmetry of the local environment of the Dy<sup>3+</sup> ions in host matrix with varying Dy<sup>3+</sup> concentration was determined by equation [8].

$$A_{21} = \frac{\oint I_2(^4F_{9/2} \rightarrow ^6H_{13/2}) d\lambda}{\oint I_1(^4F_{9/2} \rightarrow ^6H_{15/2}) d\lambda} \text{ ---- (11)}$$

where I<sub>1</sub> and I<sub>2</sub>; intensities of MD transition at 480 nm and ED transition at 575 nm respectively.

The variation of A<sub>21</sub> with varying Dy<sup>3+</sup> concentration in CdSiO<sub>3</sub> NPs was shown in **Fig.15 (c)**.

The variation of PL intensity for different concentration Dy<sup>3+</sup> ions in CdSiO<sub>3</sub> NPs was shown in **Fig.15 (c)**. From the figure, it was clearly evident that PL intensity increased with increase of concentration of Dy<sup>3+</sup> ions up to 5 mol % and afterwards it diminishes. The decrease in PL intensity was due to phenomena well known as self-concentration quenching. **Fig. 15 (d)** Shows the schematic energy-level diagram showing the excitation and emission mechanism. The CIE chromaticity diagram of the CdSiO<sub>3</sub>:Dy<sup>3+</sup> (1-11 mol %) NPs under 344 nm excitation was shown in **Fig.15 (e)**. The calculated CIE co-ordinates (x, y) were corresponds to white emission and close to the standard white chromaticity co-ordinates (x= 0.33, y= 0.33) of the National Television Standard Committee (NTSC) system [52]. In addition, correlated color temperature (CCT) of the prepared samples (**Fig.15 (f)**). The CIE and CCT values were tabulated and shown in Table 4 [53]. Also the color purity of the sample was estimated by the relation given in [54]. The colour purity (CP) values varied very close to 90 % indicate that the prepared phosphor materials may be excellent materials for white light emitting diode (WLED) applications. The obtained results specify that the present NPs may be quite useful for solid state lighting as well as advanced forensic applications. In the supplementary part of this article, LFPs stained by prepared nanophosphor were compared with commercial powders on a glass slide. Further, this part reports on the aging effects, effect of background texture, morphological changes with respect to sonication time and surfactants, PXRD patterns of pure CdSiO<sub>3</sub>, W-H plots and FTIR results as supporting results.

### <H1>4. Conclusions

A series of CdSiO<sub>3</sub>: Dy<sup>3+</sup> (1-11 mol %) NPs were fabricated by different surfactant assisted ultrasound method. The optimized product was successfully explored as efficient labeling agent for enhancing eccrine LFPs and lips prints on various surfaces including stainless steel, glass, aluminum foil, CD and different color background papers. This method was robust for revealing eccrine LFPs and lips print with high sensitivity, low background hindrance and high efficiency due to its nano size and good adherence efficiency. The PL emission spectra exhibit peaks at 480 (blue), 575 (yellow) and 637 nm (red) were attributed to <sup>4</sup>F<sub>9/2</sub>→<sup>6</sup>H<sub>15/2</sub>, <sup>4</sup>F<sub>9/2</sub>→<sup>6</sup>H<sub>13/2</sub> and <sup>4</sup>F<sub>9/2</sub>→<sup>6</sup>H<sub>11/2</sub> transitions respectively. CIE coordinate values were estimated (x=0.30889, y=0.3592) and values were very close to NTSC standard value of white emission. The present work opens up a new opportunity for the use of CdSiO<sub>3</sub>: Dy<sup>3+</sup> NPs in developing whole eccrine LFPs as well as lips prints in forensic sciences.

#### <ACK>Acknowledgement

The author Dr. H Nagabhushana thanks to DST-SERB (Project No. SR/FTP/PS-135/2010), New Delhi for the sanction of this project.

#### <REF>References

<BIBL>

- [1] H.J. Amith Yadav, B. Eraiah, H. Nagabhushana, G.P. Darshan, B. Daruka Prasad, S. C. Sharma, H.B. Premkumar, K.S. Anantharaju, and G.R. Vijayakumar,;1; ACS Sustainable Chem. Eng. 10.1021/acssuschemeng.6b01693.
- [2] J. Li, X. Zhu, M. Xue, W. Feng, R. Ma, and F. Li,;1; Inorg. Chem. 55 (2016) 10278.
- [3] P.K. Shahi, P. Singh, A.K. Singh, S.K. Singh, S.B. Rai, R. Prakash,;1; J. Colloid Interface Sci. 491 (2017) 199.
- [4] M. Wang, M. Li, M. Yang, X. Zhang, A. Yu, Y. Zhu, P. Qiu and C. Mao,;1; Nano Res. 8 (2015) 1800.
- [5] M. Saif, Magdy Shebl, A.I. Nabeel, R. Shokry, H. Hafez, A. Mbarek, K. Damak, R. Maalej,;1; M.S.A. Abdel-Mottaleb, Sens. Actuators, B. 220 (2015) 162.
- [6] B.Y. Li, X.L. Zhang, L.Y. Zhang, T.T. Wang, L. Li, C.G. Wang, Z.M. Su,;1; Dyes Pigm. 134 (2016) 178.
- [7] M. Saif, N. Alsayed, A. Mbarek, M. El-Kemary,;1; M.S.A. Abdel-Mottaleb, J. Mol. Struct. 1125 (2016) 763.
- [8] G.P. Darshan, H.B. Premkumar, H. Nagabhushana, S.C. Sharma, B. Daruka Prasad, S.C. Prashantha, R.B. Basavaraj,;1; J. Alloys Compd. 686 (2016) 577.
- [9] P. Huang, D. Tu, W. Zheng, S. Zhou, Z. Chen and X. Chen,;1; Sci. China Mater. 58 (2015) 156.
- [10] M. Zhang, Y. Ou, X. Du, X. Li, H. Huang, Y. Wen, X. Zhang,;1; J. Porous Mater. 24 (2017) 13.
- [11] A.V. Ewinga and S.G. Kazarian,;1; Analyst. 142 (2017) 257.
- [12] Y.J. Kim, H.S. Jung, J. Lim, S.J. Ryu, and J.K. Lee,;1; Langmuir. 32 (2016) 8077.
- [13] G.S. Sodhi, J. Kaur,;1; Forensic Sci. Int. 120 (2001) 172.
- [14] B. Errington, G. Lawson, S.W. Lewis, G.D. Smith,;1; Dyes Pigm. 132 (2016) 310.
- [15] L. Liu, Z. Zhang, L. Zhang, Y. Zhai,;1; Forensic Sci. Int. 183 (2009) 45.
- [16] Yan Li, Linru Xu and Bin Su,;1; Chem. Commun. 48 (2012) 4109.
- [17] D.H. Park, B.J. Park and J.M. Kim,;1; Acc. Chem. Res. 49 (2016) 1211.
- [18] J. Cui, S. Xu, C. Guo, R. Jiang, T.D. James, and L. Wang,;1; Anal. Chem. 87 (2015) 11592.

- [19] R.K. Garg, H. Kumari, R. Kaur,;1; <PL>Egypt.J</PL>. Forensic Sci. 1 (2011) 53.
- [20] J. Wang, T. Wei, X. Li, B. Zhang, J. Wang, C. Huang, and Q. Yuan,;1; Angew. Chem.126 (2014) 1642.
- [21] B.J. Jones, A.J. Reynolds, M. Richardson, V.G. Sears,;1; Sci. Justice, 50 (2010) 150.
- [22] G.P. Darshan, H.B. Premkumar, H. Nagabhushana, S.C. Sharma, S.C. Prashantha, B. Daruka Prasad,;1; J. Colloid Interface Sci. 464 (2016) 206.
- [23] G.P. Darshan, H.B. Premkumar, H. Nagabhushana, S.C. Sharma, S.C. Prashantha, H.P. Nagaswarupa, B. Daruka Prasad,;1; Dyes Pigm. 131 (2016) 268.
- [24] A. Kumar, S.P. Tiwari, A.K. Singh, K. Kumar,;1; Appl. Phys. B, 190 (2016) 1.
- [25] Mi Jung Choi, Tanya Smoother, Aiden A. Martin, Andrew M. McDonagh, Philip J. Maynard, Chris Lennard, Claude Roux,;1; Forensic Sci. Int., 173 (2007) 154.
- [26] J. Dilag, H. Kobus, A.V. Ellis,;1; Forensic Sci. Int., 187 (2009) 97.
- [27] Li Liu, S.K. Gill, Y. Gao, L.J. Hope-Weeks, K.H. Cheng, Forensic Sci. Int., 176 (2008) 163.
- [28] R.B. Basavaraj, H. Nagabhushana, B. Daruka Prasad, S.C. Sharma, S.C. Prashantha, B.M. Nagabhushana,;1; Optik. 126 (2015) 1745.
- [29] G. Ramakrishna, Ramachandra Naik, H. Nagabhushana, R.B. Basavaraj, S.C. Prashantha, S.C. Sharma, K.S. Anantharaju,;1; Optik. 127 (2016) 2939.
- [30] G. Ramakrishna, H. Nagabhushana, R.B. Basavaraj, S.C. Prashantha, S.C. Sharma, Ramachandra Naik, K.S. Anantharaju,;1; Optik. 127 (2016) 5310.
- [31] R.B. Basavaraj, H. Nagabhushana, B. Daruka Prasad, S.C. Sharma, K.N. Venkatachalaiah,;1; J. Alloys Compd., 690 (2017) 730.
- [32] Ramachandra Naik, S.C. Prashantha, H. Nagabhushana, S.C. Sharma, H.P. Nagaswarupa, K.M. Girish,;1; J. Alloys Compd. 682 (2016) 815.
- [33] Ramachandra Naik, S.C. Prashantha, H. Nagabhushana, S.C. Sharma, H.P. Nagaswarupa, K.S. Anantharaju, D.M. Jnaneshwara, K.M. Girish,;1; Dyes Pigm., 127 (2016) 25.
- [34] K. S. Suslick,;1; Sci. Am. 260 (1989) 80.
- [35] Jin Ho Bang, Kenneth S. Suslick,;1; Adv. Mater. 22 (2010) 1039.
- [36] R.B. Basavaraj, H. Nagabhushana, B. Daruka Prasad, G.R. Vijayakumar,;1; Ultrason Sonochem. 34 (2017) 700.
- [37] M. Venkataravanappa, H. Nagabhushana, G.P. Darshan, B. Daruka Prasad, G.R. Vijayakumar, H.B. Premkumar,;1;Udayabhanu, Ultrason. Sonochem. 33 (2016) 226.
- [38] M. Venkataravanappa, H. Nagabhushana, B. Daruka Prasad, G.P. Darshan, R.B. Basavaraj, G.R. Vijayakumar,;1; Ultrason Sonochem. 34 (2017) 803.
- [39] X. Qu, L. Cao, W. Liu, G. Su,;1; J. Alloys Compd. 533 (2012) 83.
- [40] C. Manjunatha, D.V. Sunitha, H. Nagabhushana, B.M. Nagabhushana, S.C. Sharma, R.P.S. Chakradhar,;1; Spectrochim. Acta, Part A 93 (2012) 140.
- [41] X. Qu, L. Cao, W. Liu, G. Su, H. Qu, C. Xu,;1; J. Alloys Compd. 484 (2009) 641.
- [42] H. Nagabhushana, D.V. Sunitha, S.C. Sharma, B. Daruka Prasad, B.M. Nagabhushana, R.P.S. Chakradhar,;1; J. Alloys Compd. 595 (2014) 192.
- [43] B.M. Manohara, H. Nagabhushana, K. Thyagarajan, Daruka Prasad B, S.C. Prashantha, S.C. Sharma, B.M. Nagabhushana,;1; J. Lumin. 161 (2015) 247.
- [44] J. Kasprzak,;1;Forensic Sci. Int., 46 (1990) 145.
- [45] A. Castello, M. Alvarez-Segui, F. Verd, Forensic Sci. Int., 155 (2005) 185.
- [46] L.V. Krishna Reddy, Journal of Advanced Oral Research, 2 (2011) 17.
- [47] P. Mishra, R.S. Yadav, A.C. Pandey,;1; Ultrason. Sonochem. 17 (2010) 560-565.

- [48] K. Munirathnam, G.R. Dillip, S. Chaurasia, S.W. Joo, B.D.P Raju, N.J. Sushma, J. Mol. Struct. 118 (2016) 117.
- [49] Neharika, V. Kumar, V.K. Singh, J. Sharma, O.M. Ntwaeaborwa, H.C. Swart,;1; J. Alloys Compd. 688 (2016) 939.
- [50] H. Nagabhushana, R.B. Basavaraj, B. Daruka Prasad, S.C. Sharma, H.B. Premkumar, Udayabhanu, G.R. Vijayakumar,;1; J. Alloys Compd. 669 (2016) 232.
- [51] K. Mondal, P. Kumari, J. Manam,;1; Curr. Appl Phys. 16 (2016) 707.
- [52] Publication CIE no 17.4 (1987) International Lighting Vocabulary, Central Bureau of the Commission Internationale de L 'Eclairage, <PL>Vienna, Austria</PL>.
- [53] C.S. McCamy,;1; Color Res. Appl., 17 (1992) 142.
- [54] T. Smith, J. Guild,;1; Transactions of Optical Soc. 33 (1931) 75.

</BIBL>

<Figure>Fig. 1. Flow chart of the present study.

<Figure>Fig. 2. Schematic representation which shows the method to obtain eccrine latent finger prints using CdSiO<sub>3</sub>:Dy<sup>3+</sup> NPs. (a) Taking the finger print of healthy individual on a glass slide (b) smooth brushing and spreading of prepared phosphor NPs (c) Observing the presence of well-defined FPs on various kinds of materials (d) Taking photograph of the FPs (e) photographs of the FPs under UV light illumination.

<Figure>Fig. 3. Eccrine LFPs obtained by starch-CdSiO<sub>3</sub>:Dy<sup>3+</sup> NPs on: (a) glass, (b) stainless steel sheet, (c) aluminum foils, (d) mobile screen (e) compact disk, (f) laptop, (g) laptop screen and (h) calling bell.

<Figure>Fig. 4. Eccrine LFPs stained by CdSiO<sub>3</sub>:Dy<sup>3+</sup> NP on various magazine covers with different background colour and letters.

<Figure>Fig. 5. Comparison of the imaging of eccrine latent finger prints with different surfactants (a) CTAB, (b) Starch, (c) PEG, and (d) SDS assisted ultrasound synthesized CdSiO<sub>3</sub>:Dy<sup>3+</sup> nano material.

<Figure>Fig. 6. Some identified minutia ridges of the LFPs were shown in the left side of the figure. For comparison, eccrine LFPs stained by (a) commercial (TiO<sub>2</sub>) powder and (b)

CdSiO<sub>3</sub>:Dy<sup>3+</sup> NPs (right) were shown. Figs. (c) - (e) shows the part of the two FPs after post processed.

<Figure>Fig. 7. LFPs taken after staining by CdSiO<sub>3</sub>:Dy<sup>3+</sup> NPs on various surfaces

(a) - (c) porous paper bar codes, (d) pet bottle and (e) - (f) non- porous coins.

<Figure>Fig. 8 (A). Three different latent lips print enhanced on the surface of glass stained by CdSiO<sub>3</sub>:Dy<sup>3+</sup> nano material. (B) Various lip print patterns with different grooves demonstration.

<Figure>Fig. 9 (A). SEM images of CdSiO<sub>3</sub>:Dy<sup>3+</sup> (5 mol %) nano material with different concentration of CTAB (5, 10, 15, 20, 25 and 30 ml) with 6 h of ultrasonic irradiation time. (B) SEM images of CdSiO<sub>3</sub>:Dy<sup>3+</sup> (5 mol %) nano material with different concentration of starch (5, 10, 15, 20, 25 and 30 ml) with 6 h of ultrasonic irradiation time.

<Figure>Fig. 10. Schematic representation of CdSiO<sub>3</sub> nanomaterials in the presence of starch.

<Figure>Fig. 11 (A). SEM images of CdSiO<sub>3</sub>:Dy<sup>3+</sup> (5 mol %) nano material with different concentration of SDS (5, 10, 15, 20, 25 and 30 ml) with 6 h of ultrasonic irradiation time. (B) SEM images of CdSiO<sub>3</sub>:Dy<sup>3+</sup> (5 mol %) nano material with various pH values (5, 7, 9, and 11) with 6 h of ultrasonic irradiation time and starch (25 ml).

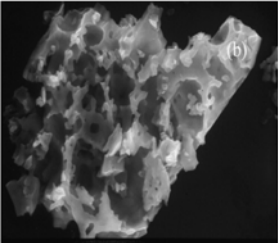
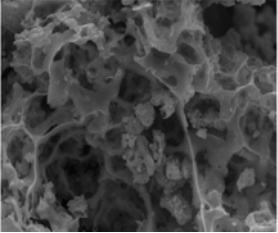
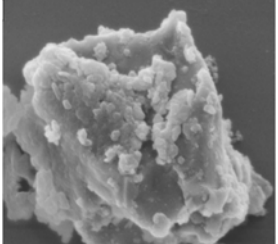
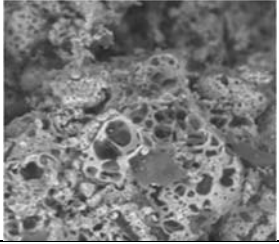
<Figure>Fig. 12. TEM images of optimized CdSiO<sub>3</sub>:Dy<sup>3+</sup> (5 mol %) nano material prepared with (a) CTAB (b) Starch (c) SDS (d) PEG surfactants and 6 h of ultrasonic irradiation time.

<Figure>Fig. 13. PXRD patterns of pure CdSiO<sub>3</sub> nano material synthesized by mechanical stirring and ultrasonic method with 6 h of stirring and ultrasonic irradiation time.

<Figure>Fig. 14 (a). Diffuse reflectance spectra of undoped and CdSiO<sub>3</sub>: Dy<sup>3+</sup> (1 – 11 mol %), (b) Energy band gap plots of prepared nano material with 6 h ultrasound irradiation with starch (25 ml).

<Figure>Fig. 15. (a) Excitation, (b) Emission, (c) PL Intensity V/s dopant concentration and asymmetric ratio and (d) energy level diagram of  $Dy^{3+}$  ions in  $CdSiO_3$  host synthesized with 6 h ultrasound irradiation with starch (25 ml). (e) CIE and (f) CCT diagrams of  $Dy^{3+}$  (1 – 11 mol %) doped  $CdSiO_3$  nano material prepared with 6 h ultrasound irradiation with starch (25 ml).

Table. 1. Method of preparation, formation temperature and morphology of the product obtained in pure and doped  $CdSiO_3$  nano material.

Method of Preparation	Formation temperature (°C)	Shape of the product	Reference	Morphology
Sol-gel	1050	Irregular	Xiaofei Qu et al	
Solution combustion	800	Porous nature	Manjunatha et al	
Sol-gel	900	Irregular	Xiaofei Qu et al	
Solution combustion	800	Fluffy-agglomerated	Nagabhushana et al	

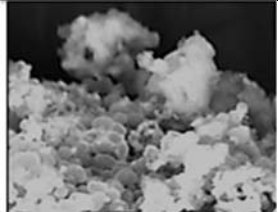
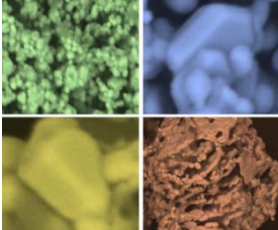
Solution combustion	900	Irregular	Manohara et al	
Sonochemical	800	Spherical, hexagonal, pyramidal, network like	Present work	

Table. 2. List of chemicals and surfactants used in the present study.

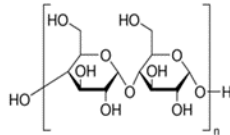
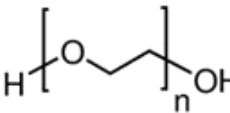
Chemicals	Linear formula	Molecular weight (g/mol)	Details of surfactant			
			Surfactant	Linear formula	Structure	Molecular weight (g/mol)
Cadmium nitrate tetrahydrate	$\text{Cd}(\text{NO}_3)_2 \cdot 4\text{H}_2\text{O}$	308.08	Starch	$(\text{C}_6\text{H}_{10}\text{O}_5)_n$		342.30
Tetraethyl orthosilicate	$\text{Si}(\text{OC}_2\text{H}_5)_4$	208.33	Poly(ethylene glycol) (PEG)	$\text{H}(\text{OCH}_2\text{C}_2\text{H}_4)_n\text{OH}$		200
Dysprosium (III) nitrate hydrate	$\text{Dy}(\text{NO}_3)_3 \cdot x\text{H}_2\text{O}$	348.51	Cetrimonium bromide (CTAB)	$\text{CH}_3(\text{CH}_2)_{11}\text{N}(\text{Br})(\text{CH}_2)_3$	<remove picture pageno 23>	364.45
			Sodium dodecyl sulfate (SDS)	$\text{CH}_3(\text{CH}_2)_{11}\text{OSO}_3\text{Na}$	<remove picture pageno 23>	288.38

Table. 3. Estimated crystallite size, micro strain, energy gap (Eg), refractive index (n) and morphology of the CdSiO<sub>3</sub>: Dy<sup>3+</sup> nano material prepared under various reaction parameters.

Reaction Parameter		Crystallite size (nm)		Micro strain (x 10 <sup>-3</sup> )	Energy gap (eV)	Refractive index (n)	Morphology
		D-S approach	W-H approach				
Surfactant	Starch	18	19	0.95	5.28	1.7078	Hexagonal disk
	PEG	24	23	1.11	5.25	1.7114	Porous
	CTAB	32	29	1.14	5.23	1.7133	Flakes
	SDS	40	38	1.25	5.21	1.7233	Spherical
Sonication time (h)	1	44	43	1.14	5.32	1.7035	
	2	41	39	1.10	5.41	1.6939	
	3	29	32	1.12	5.42	1.6929	Sponge like
	5	27	29	1.27	5.45	1.6897	
	6	19	17	1.34	5.53	1.6814	
pH value	1	51	48	1.12	5.23	1.7133	
	3	49	53	2.13	5.25	1.7111	
	7	46	48	2.45	5.27	1.7089	Chain like network
	9	44	47	2.46	5.31	1.7041	
	11	41	43	2.60	5.34	1.7013	
	13	40	39	2.62	5.35	1.7003	
Sonication power (kHz)	20	19	22	1.42	5.42	1.6929	
	24	21	25	1.52	5.39	1.6960	
	28	24	28	1.56	5.36	1.6992	Irregular flakes
	32	33	31	1.60	5.31	1.7046	
	36	38	36	1.72	5.26	1.7100	
	40	41	40	1.95	5.25	1.7111	

Table. 4. Photometric characteristics of Dy<sup>3+</sup> (1- 11 mol %) doped CdSiO<sub>3</sub> nano materials prepared with 6 h ultrasound irradiation and starch (25 ml).

Dy <sup>3+</sup> (mol %)	CdSiO <sub>3</sub> :Dy <sup>3+</sup>			
	X	Y	CCT (K)	CP (%)



1	0.3213	0.3066	6148	91.02
3	0.3113	0.3066	6793	92.32
5	0.3213	0.3166	6098	95.12
7	0.3131	0.3198	6551	88.16
9	0.3206	0.3074	6186	90.54
11	0.3152	0.3214	4212	91.25

TDENDOFDOCTD